THE JOURNAL OF BIOLOGICAL CHEMISTRY VOL. 287, NO. 52, pp. 43840–43852, December 21, 2012

Functional Genetic Variants of the Catecholamine-Release-Inhibitory Peptide Catestatin in an Indian Population

ALLELE-SPECIFIC EFFECTS ON METABOLIC TRAITS[*S]

Received for publication, August 4, 2012, and in revised form, October 19, 2012 Published, JBC Papers in Press, October 26, 2012, DOI 10.1074/jbc.M112.407916

Bhavani S. Sahu[‡], Jagan M. Obbineni[‡], Giriraj Sahu[‡], Prasanna K. R. Allu[‡], Lakshmi Subramanian[‡], Parshuram J. Sonawane[‡], Pradeep K. Singh[§], Binu K. Sasi[‡], Sanjib Senapati[‡], Samir K. Maji[§], Amal K. Bera[‡], Balashankar S. Gomathi[¶], Ajit S. Mullasari[¶], and Nitish R. Mahapatra[‡1]

From the [‡]Department of Biotechnology, Indian Institute of Technology Madras, Chennai 600036, India, the [§]Department of Biosciences and Bioengineering, Indian Institute of Technology Bombay, Mumbai 400076, India, and the [¶]Institute of Cardiovascular Diseases, Madras Medical Mission, Chennai 600037, India

Background: Catestatin is emerging as a novel regulator of cardiovascular/metabolic functions.
Results: We discovered a common amino acid substitution variant of catestatin that caused profound changes in plasma catecholamines, glucose, and lipid levels.
Conclusion: Naturally occurring variants of catestatin peptide seem to alter the risk for metabolic syndrome.
Significance: These findings provide new insights into the mechanism of metabolic diseases in humans.

Catestatin (CST), a chromogranin A (CHGA)-derived peptide, is a potent inhibitor of catecholamine release from adrenal chromaffin cells and postganglionic sympathetic axons. We resequenced the CST region of *CHGA* in an Indian population ($n = 1010$) and detected two amino acid substitution variants: G364S and G367V. Synthesized CST variant peptides (*viz.* CST-Ser-364 and CST-Val-367) were significantly less potent than the wild type peptide (CST-WT) to inhibit nicotine-stimulated catecholamine secretion from PC12 cells. Consistently, the rank-order of blockade of nicotinic acetylcholine receptor (nAChR)-stimulated inward current and intracellular Ca^{2+} rise by these peptides in PC12 cells was: CST-WT > CST-Ser-364 > CST-Val-367. Structural analysis by CD spectroscopy coupled with molecular dynamics simulations revealed the following order of α-helical content: CST-WT > CST-Ser-364 > CST-Val-367; docking of CST peptides onto a major human nAChR subtype and molecular dynamics simulations also predicted the above rank order for their binding affinity with nAChR and the extent of occlusion of the receptor pore, providing a mechanistic basis for differential potencies. The G364S polymorphism was in strong linkage disequilibrium with several common *CHGA* genetic variations. Interestingly, the Ser-364 allele (detected in ~15% subjects) was strongly associated with profound reduction (up to ~2.1-fold) in plasma norepinephrine/epinephrine levels consistent with the diminished nAChR desensitization-blocking effect of CST-Ser-364 as compared with CST-WT. Additionally, the Ser-364 allele showed strong associations with elevated levels of plasma triglyceride and glucose levels. In conclusion, a common *CHGA* variant in an Indian population influences several biochemical parameters relevant to cardiovascular/metabolic disorders.

Chromogranin A (CHGA[2]; OMIM 118910) is the major protein co-stored and co-released with catecholamines from secretory granules of chromaffin cells and adrenergic neurons (1–4). CHGA plays a key role in the biogenesis of catecholamine storage vesicles (5–7). CHGA also acts as a prohormone and undergoes proteolytic cleavage to generate several peptides that have been implicated for regulation of cardiovascular/metabolic functions; examples of such bioactive peptides include vasostatin-I (human $CHGA_{1-76}$, a vasodilator and suppressor of myocardial inotropy/lusitropy), pancreastatin (PST; human $CHGA_{250-301}$, a dysglycemic hormone), catestatin (CST; human $CHGA_{352-372}$, a potent inhibitor of catecholamine secretion and cardio-suppressive agent), and serpinin (human $CHGA_{411-436}$, a novel myocardial β-adrenergic-like agonist) (8–13).

Studies by us and others revealed that CST specifically acts at the neuronal nicotinic acetylcholine receptor (nAChR) to regulate catecholamine secretion into the circulation (14–17). Interestingly, plasma CST concentration is diminished not only in established hypertensive patients but also in their still-normotensive offspring, suggesting a pathogenic role for this peptide in hypertension (18). Consistently, mice lacking CST (generated by systemic deletion of its precursor CHGA molecule) displayed severe hypertension that could be rescued by administration of human CST peptide (7). Very recently, CST has been reported to act as an insulin-sensitizing agent (perhaps via inhibition of gluconeogenesis) as well as to regulate lipogenesis, lipolysis, and fatty acid oxidation (4, 19). Thus, CST is emerging as a novel regulator of cardiovascular/metabolic functions.

Resequencing of the *CHGA* locus in a Southern California population ($n = 180$ subjects) led to the identification of three non-synonymous variants in the CST domain: G364S, P370L,

* This work was supported by a grant (BT/PR9546/MED/12/349/2007) from the Department of Biotechnology, Government of India (to N. R. M., A. S. M., and B. S. G.).
[S] This article contains supplemental Table S1 and Figs. S1 and S2.
[1] To whom correspondence should be addressed. Tel.: 91-44-2257-4128; Fax: 91-44-2257-4102; E-mail: nmahapatra@iitm.ac.in.

[2] The abbreviations used are: CHGA, chromogranin A; PST, pancreastatin; CST, catestatin; ACh, acetylcholine; nAChR, neuronal nicotinic acetylcholine receptor; SNP, single nucleotide polymorphism; TFE, 2,2,2-triflouroethanol; contig, group of overlapping clones; ANOVA, analysis of variance.

and R374Q (20). However, the status of genetic variants of CST in ethnically /geographically different human populations remains unclear. Importantly, these CST variants display significantly different potencies toward inhibition of nAChR-evoked catecholamine secretion from sympathochromaffin cells (15). Moreover, the Ser-364 allele was associated with blood pressure variation and prediction of risk for hypertension, especially in men (21). We hypothesize that replication studies in subjects with different ancestries may confirm/yield novel associations of CST variants with cardiovascular disease states.

In this study we probed for genetic variations in the CST region of *CHGA* in an Indian population ($n = 1010$ subjects) and discovered two non-synonymous single nucleotide polymorphisms (SNPs) that resulted in two variants, G364S and G367V; although the Ser-364 variant occurred in ~15% of the population, the Val-367 variant was novel and rare. Both of these CST variants discovered in the Indian population (*viz.* CST-Ser-364 and CST-Val-367) showed diminished antagonism to nAChR than the wild type peptide (CST-WT). We undertook a multidisciplinary approach to unravel the molecular mechanism of differential potency/efficacy of these CST peptides. This study also revealed that carriers of Ser-364 allele had significantly altered plasma levels of several biochemical parameters (including glucose, lipids, and catecholamines) relevant to metabolic syndrome.

EXPERIMENTAL PROCEDURES

Human Subjects—We recruited unrelated 1010 volunteer individuals from urban Chennai cosmopolitan population at the Madras Medical Mission hospital. Each subject gave informed, written consent; this study was approved by the Institute Ethics Committees at Madras Medical Mission hospital and Indian Institute of Technology Madras. Demographics (age, gender), physical (height, weight, body mass index), physiological (systolic blood pressure, diastolic blood pressure, mean arterial pressure, heart rate, left ventricular dimension at end systole, left ventricular dimension at end diastole) parameters, and medical history (including whether currently taking antihypertensive medications, family history of cardiovascular and renal disease states) data were collected from the subjects. The average age of the subjects was ~39 years. The overall study population consisted of 550 essential hypertensives (systolic blood pressure >140 mm Hg or diastolic blood pressure >90 mm Hg or a history of hypertension and antihypertensive treatment; no history of kidney disease or diabetes) and 460 unmedicated normotensives (with no history of hypertension or kidney disease or diabetes). Blood pressure was measured on the sitting position by experienced nursing staff using a brachial oscillometric cuff, and triplicate values were averaged. About 94% of the hypertensive subjects received antihypertensive medications including beta blockers, angiotensin convertase enzyme inhibitors, angiotensin II receptor blocker, and calcium channel blockers. Blood samples were collected by peripheral venipuncture in EDTA-containing tubes for isolation of genomic DNA; plasma samples were also collected, aliquoted, and stored at −80 °C for assaying various biochemical parameters.

Discovery of Genetic Polymorphisms at the CHGA Locus—Genomic DNA was isolated from EDTA-anticoagulated blood samples ($n = 1010$) using FlexiGene DNA kit (Qiagen) according to the manufacturer's protocol. The following primers were used to amplify the CST region in the exon 7 of *CHGA* (NCBI accession number NM_001275): CHGA-9236-FP (5′-CCCATTCTCCTGCTCTTGCC-3′) and CHGA-9750-RP (5′-TCCCGCCCCATACCAACCTC-3′). The target amplicon (579 bp) was amplified by using Phusion™ high fidelity DNA polymerase and dNTPs (New England Biolabs). The routine PCR reaction mixture (20 μl) consisted of the following (final concentrations): 1.5 mM $MgCl_2$, 0.4 mM each dNTP, 1 mM concentrations of each primer, 20 ng of template DNA, 0.4 unit of the DNA polymerase. The PCR protocol began with a 98 °C denaturation step for 2 min followed by a touchdown program (98 °C denaturation step for 30 s followed by an initial annealing temperature of 70 °C for 30 s, subsequently run down to 55 °C at −1 °C/cycle and 72 °C extension step for 1 min) followed by a uniform three-step amplification profile (98 °C denaturation step for 30 s, 54 °C annealing step for 30 s, 72 °C extension step for 1 min) for another 23 cycles, then 72 °C for 10 min, and finally held at 4 °C.

The PCR products were visualized on ethidium bromide-stained agarose gels, purified by using PCR purification columns (QIAquick PCR Purification kit, Qiagen) and sequenced using the forward primer CHGA-9236-FP (mentioned above). Polymorphisms were detected and confirmed from chromatograms. To confirm any ambiguity about a polymorphism, re-sequencing of the sample was carried out using the reverse primer CHGA-9750-RP (mentioned above). A subset ($n = 333$) of those DNA samples were subjected to genotyping of *CHGA* promoter SNPs by PCR amplification and sequencing using the following primers: CHGApro-1185-FP (5′-CAGGCGTGAG-CACAGGTGTG-3) and CHGApro+76-RP (5′-TCCGTCT-GTCGGTCGATCC-3′).

Synthesis of CST Peptides—The CST wild type (CST-WT, SSMKLSFRARAYGFRGPGPQL) and two variant peptides (CST-Ser-364, SSMKLSFRARAY**S**FRGPGPQL; CST-Val-367, SSMKLSFRARAYGFR**V**PGPQL) were synthesized by solid phase method and purified to >95% homogeneity by GenPro Biotech, New Delhi, India. Authenticity and purity of these peptides were verified by analytical high performance liquid chromatography and mass spectrometry.

Cell Culture Conditions—Rat pheochromocytoma PC12 cells were obtained from the laboratory of Dr. Daniel O'Connor, University of California San Diego. The cells were cultured in Dulbecco's modified Eagle's high glucose medium with 10% horse serum, 5% fetal bovine serum, 100 units/ml penicillin G, and 100 μg/ml streptomycin (Invitrogen) as described earlier (17).

Catecholamine Secretion Experiments—Catecholamine secretion from PC12 cells grown in 6-well plates and prelabeled with 0.5 μCi of L-[7-^{3}H]norepinephrine was assayed as described previously (14). In brief, the cells were stimulated by nicotine (60 μM) in the presence/absence of each CST peptide (*viz.* CST-WT, CST-Ser-364, CST-Val-367), and the secretion media and cell lysates were assayed for [^{3}H]norepinephrine counts in a PerkinElmer Life Sciences Tricarb™ liquid scintillation coun-

ter. The results were expressed as % of cell total [^{3}H]norepinephrine released under various conditions. The net secretion in each experiment was calculated as stimulated release minus basal (unstimulated) release of [^{3}H]norepinephrine.

Assay for Desensitization of Nicotine-evoked Catecholamine Release—An assay to test inhibition of desensitization of nicotine-stimulated catecholamine secretion by the CST peptides was carried out as described previously with minor modifications (15). Briefly, PC12 cells in 6-well plates were preloaded with 0.5 μCi of [^{3}H]norepinephrine and stimulated with nicotine (30 μM) for 10 min in the presence or absence of increasing concentrations (0.1–10 μM) of each CST peptide (*viz.* CST-WT, CST-Ser-364, and CST-Val-367). Cells were then washed twice (10 min each) with secretion buffer and restimulated with nicotine (30 μM) for another 10 min. Measurement of norepinephrine counts released in the media and in the cells were carried out as described earlier (15). Data were expressed as % increments in catecholamine secretion due to CST peptides over the desensitized condition (without CST peptides).

Electrophysiology Experiments—Whole-cell patch clamp experiments on PC12 cells were carried out with/without acetylcholine (ACh; 100 μM, Sigma) in the presence/absence of CST peptides (*viz.* CST-WT, CST-Ser-364, and CST-Val-367) as described earlier (17). Nerve growth factor (100 ng/ml)-differentiated PC12 cells clamped at −80 mV were treated with ascending concentrations of each peptide (0.1, 0.25, 1.0, 2.5, 5.0, and 10 μM) to block the ACh-evoked inward current. Data were expressed as blockade of inward current with respect to control (without peptide).

Measurement of Intracellular Calcium Concentrations—Intracellular free calcium concentration ($[Ca^{2+}]_i$) in PC12 cells was measured by ratiometric method using Fura 2-AM dye (Invitrogen) as described previously (17). Nicotine (200 μM, Sigma)-induced calcium rise was measured in the presence or absence of CST-WT, CST-Ser-364, and CST-Val-367 peptides (at 5 μM final concentration). Nerve growth factor-treated PC12 cells were preincubated with a CST peptide for 2 min followed by its co-application with nicotine. The rise in $[Ca^{2+}]_i$ value in the presence of each peptide was compared with the corresponding control (basal level).

Circular Dichroism (CD) Spectroscopic Analysis of the CST Peptides—The secondary structures of CST-WT, CST-Ser-364, and CST-Val-367 peptides were analyzed by CD spectroscopy as described previously (17) with some modifications. In brief, peptides were dissolved at the final concentration of 50 μM phosphate-buffered saline (PBS), pH 7.4, and spectra were recorded over the wavelength range of 198–260 nm. Additionally, spectra were also recorded in the presence of various 2,2,2-triflouroethanol (TFE) concentrations (v/v) (10, 30, 50, 70, and 90% in PBS) at 50 μM peptide concentration. The relative quantities of random coil, α-helix, β-sheet, and β-turn in the CST peptides were determined by deconvolution of CD data using the CDPro software package.

Computational Analysis of Structures of CST Peptides and Their Interactions with nAChR—Computational analyses to probe the structural variations among CST variants in our study population as well as interactions of these peptides with nAChR were carried out as described previously (17). In brief, the three-dimensional nuclear magnetic resonance structure of CST-WT (PDB ID 1LV4) (22) was equilibrated in water using AMBER force field (23), and models of the variants (*viz.* CST-Ser-364, CST-Val-367) were obtained by introducing the respective mutations using the mutagenesis wizard in PyMOL (The PyMOL Molecular Graphics System). The peptides were then simulated for 180 ns in water, and the molecular dynamics trajectories were visualized in Visual Molecular Dynamics (VMD) (24) using home-built codes to generate their time-averaged structures. The representative structures were docked on the extracellular domain of human $\alpha_3\beta_4$ nAChR structure using Autodock 3.05 (25); the $\alpha_3\beta_4$ nAChR structure was generated by homology modeling based on the 4.0 Å resolution structure of *Torpedo marmorata* nAChR (PDB ID 2BG9) (26). The extracellular and transmembrane domains of the modeled $\alpha_3\beta_4$ nAChR structure were embedded in an equilibrated lipid bilayer (composed of 1-palmitoyl-2-oleoyl-*sn*-glycerol phospatidylcholine, 1-palmitoyl-2-oleoyl-*sn*-glycerol phosphatidic acid, and cholesterol in the ratio of 3:1:1) as functional nAChRs require the presence of lipid and cholesterol molecules in the vicinity of the receptor molecules (27, 28), and the structural stability of the receptor in the bilayer was ascertained. After docking of the final structures CST-WT, CST-Ser-364, and CST-Val-367 on the human $\alpha_3\beta_4$ nAChR structure, molecular dynamics simulation was carried out at 300 K temperature and 1 atm of pressure using NAMD2.6 package (29). Final simulated peptide-receptor complexes were then picked for various analyses. The peptide receptor interactions for the three CST peptides were calculated using the Protein Interactions Calculator web server (30) for different types of interactions, *viz.* hydrophobic, ionic, hydrogen bonding, and aromatic-aromatic interactions. Interaction energy of the stable, bound peptide after achieving flexibility in MD simulations was evaluated using Autodock 3.05 energy scoring function. We also calculated the percentage occlusion of the pore by each CST peptide by using the HOLE program (31).

Estimation of Biochemical Parameters—Glucose (random blood sugar), cholesterol, urea, creatinine, hemoglobin, sodium, and potassium levels in the plasma were determined by standard biochemical assays. Catecholamine (norepinephrine and epinephrine) levels in the plasma samples were quantified by a radioimmunoassay kit (LDN). Briefly, norepinephrine and epinephrine from ~200 μl of plasma were extracted using a *cis*-diol-specific affinity gel, acylated to *N*-acylnorepinephrine, and *N*-acylepinephrine, respectively, and eluted in 200 μl of 25 mM hydrochloric acid. The eluted samples were then enzymatically converted to *N*-acylnormetanephrine and *N*-acylmetanephrine and detected by radioimmunoassay as per the manufacturer's protocol. ^{125}I radioactivity counts of the samples were determined by a PerkinElmer Life Sciences Wizard™ gamma counter. A series of standards were run along with the samples to estimate the absolute amounts of the catecholamines in the samples, and the results were expressed in pg/ml.

Data Presentation and Statistical Analysis—The experimental data are representative of 4–5 separate experiments. Results from cell culture studies are expressed as the mean ± standard error of mean (S.E.) values from replicate cells/wells as indi-

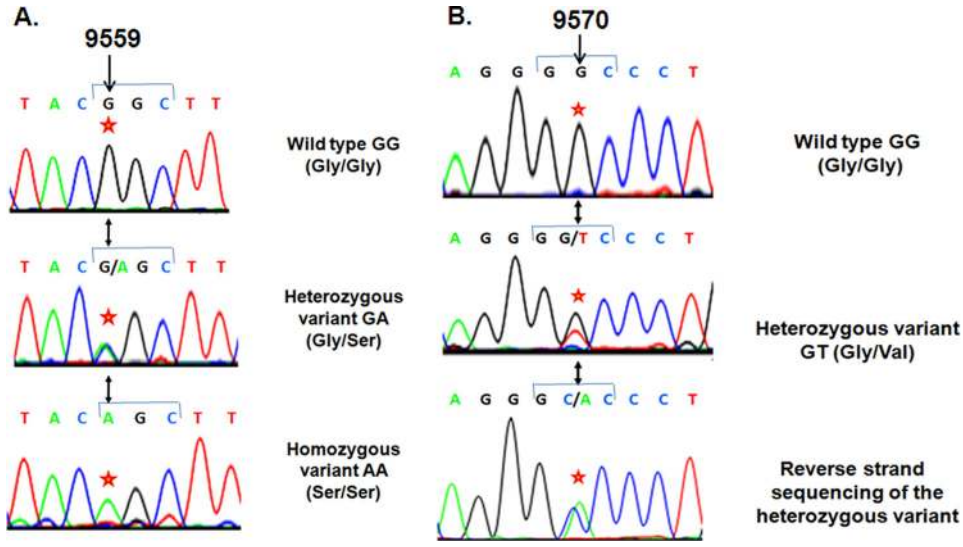

FIGURE 1. **Discovery of the natural amino acid variants of the endogenous anti-hypertensive peptide catestatin.** 1010 subjects were re-sequenced across the exon 7 of the chromogranin A gene, including the catestatin region. Representative chromatograms are shown for two variants discovered in catestatin. *Panel A*, shown is the G364S variant. Wild type GG (Gly/Gly), heterozygous variant G/A (Gly/Ser), and homozygous variant AA (Ser/Ser) at 9559 bp position are shown. The codon 364 (G364S) numbering is with reference to the mature protein, and it is equivalent to codon 382 in the preprotein that contains the signal peptide. Here, the first nucleotide (indicated by an *) of the codon GGC (in the wild type) is altered to AGC (in the variant) that would alter the amino acid glycine to serine. *Panel B*, shown is the G367V variant. Wild type GG (Gly/Gly) and heterozygous variant G/T (Gly/Val) at the 9570-bp position are shown. Reverse-strand sequencing of the heterozygous variant confirmed the genetic variation. Here, the second nucleotide (indicated by an *) of the codon GGC (in the wild type) is altered to GTC (in the variant), which would alter the amino acid glycine to valine. The base numbers refer to position in the chromogranin A sequence downstream from the cap (transcription initiation) site.

cated in the respective figure legends. To evaluate the effects of CST peptides and their various concentrations on the nAChR signaling, two-way ANOVA and/two-tailed *t* tests as appropriate were carried out. Phenotypic parameters of the study subjects were expressed as the mean ± S.E. Association studies were carried out for Gly/Gly, Gly/Ser, and Ser/Ser genotypes with various phenotypic data (that excluded abnormal outliers by quartile analysis) where available. To evaluate the significance of allele-specific associations, inferential statistics (one-way ANOVA with post hoc tests or Levene's test for equality of variances and *t* test for equality of means, as appropriate) were performed. Statistical associations between genotypes and phenotypes were also tested separately in hypertensive and normotensive subjects. The blood pressure data were adjusted for antihypertensive treatments using the method of Cui *et al.* (32) as our study population contained a large proportion of hypertensive subjects. Statistical analyses were performed using SPSS software (SPSS Inc., Chicago, IL). A p value of ≤ 0.05 was chosen for statistical significance between the groups.

RESULTS

Discovery of Non-synonymous SNPs in the CST Domain of CHGA—To probe for genetic polymorphisms in the CST ($CHGA_{352-372}$) region in an Indian population, we resequenced the flanking *CHGA* locus in 1010 unrelated individuals (*i.e.* 2020 chromosomes). About 15.0% of this study population carried A at the 9559-bp position (downstream from the transcription initiation site) in the genomic contig instead of G in one or both chromosomes (G/G = 858, G/A = 144, A/A = 8), causing substitution of Gly (codon **G**GC) by Ser (codon **A**GC) at the 364-residue position of the parent protein CHGA (Fig. 1; Table 1). The genotype frequencies (Gly-364, 92.08%; Ser-364, 7.92%) were in Hardy-Weinberg equilibrium ($\chi^2 = 0.515$, $p = 0.473$). This G9559A SNP (*i.e.* G364S variant; rs9658667) was previously detected in a Southern California population ($n = 180$ individuals) (20) wherein the Ser-364 allele occurred at ~3.1% frequency (*i.e.* at ~2.6-fold lower allele frequency than this Indian study population). Additionally, about 0.099% of the present study population carried T at the 9570-bp position instead of G in one chromosome, causing substitution of Gly (codon G**G**C) by Val (codon G**T**C) (Fig. 1, Table 1). This variant, denoted as G367V (rs200576557) is a rare one that was not detected in the Southern California population. To confirm this substitution, we carried out reverse-strand sequencing that revealed the presence of A at the opposite strand (Fig. 1).

Differential Antagonism to nAChR by Human CST Variants—Although CST is emerging as a multifunctional peptide (4, 33), the most well understood function of this peptide (human and bovine orthologue) is its non-competitive antagonistic action on nAChR (11, 14, 16, 17). Therefore, we investigated whether the CST variants discovered in our study population display differential nAChR inhibitory effects.

First, we measured nicotine (60 μM)-induced [^{3}H]norepinephrine secretion from PC12 cells in the presence/absence of ascending concentrations (0.1- 5.0 μM) of each of the three human CST variants (*viz.* CST-WT, CST-Ser-364, and CST-Val-367). Each peptide blocked the nicotine-stimulated secretion in a concentration-dependent manner (Fig. 2). Interestingly, the CST peptides significantly differed in their secretion-inhibitory effects, CST-WT being the most potent, whereas CST-Val-367 was the least potent (Fig. 2).

Second, we sought to test the effect of these peptides on ACh-evoked inward current in these cells. Small pulses (3 s) of ACh (100 μM) were applied to voltage-clamped PC12 cells to elicit inward current (I_{ACh}) before, during, and after application

TABLE 1

Sequence variants of human catestatin in an Indian population with allelic distribution

The variant amino acids are shown in bold.

Human CST variants in an Indian population (n = 1010)	dbSNP ID	Allele frequency
		%
CST-WT, SSMKLSFRARAYGFRGPGPQL		92.08
CST-Ser-364, SSMKLSFRARAY**S**FRGPGPQL	rs 9658667	7.92
CST-Val-367, SSMKLSFRARAYGFR**V**PGPQL	rs 200576557	0.05

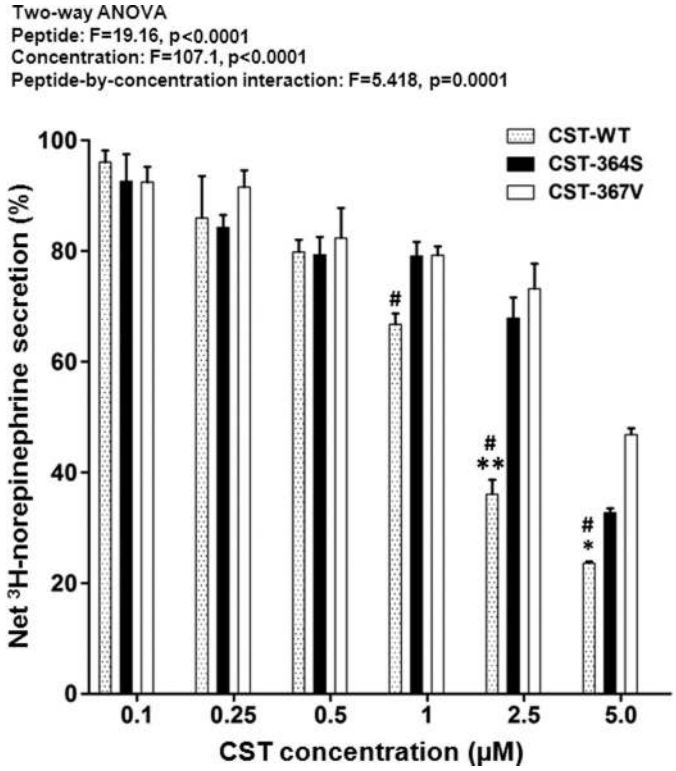

FIGURE 2. **Differential inhibition of catecholamine secretion by CST variants in an Indian population.** PC12 cells cultured in poly L-lysine-coated 12-well plates were preloaded with [^{3}H]norepinephrine and treated with 60 μM nicotine without/with ascending concentrations (0.1–5 μM) of CST peptides. Each data point represents the mean ± S.E. of three separate wells. The control (100%) is norepinephrine secretion when challenged with 60 μM nicotine alone without peptide. Results of two-way ANOVA are shown, factoring for the effects of peptide, concentration, and peptide-by-concentration interaction on the net [^{3}H]norepinephrine secretion. * and ** indicate $p < 0.05$ and $p < 0.01$ with respect to CST-Ser-364, whereas # indicates $p < 0.01$ with respect to CST-Val-367 (by two-tailed t test).

of each CST peptide. Representative I_{ACh} traces for each CST peptide are shown in Fig. 3, *panel A*, *B*, and *C*); in each case the inhibitory effect was reversible after wash out of the peptide (*third trace from the left*) indicating the specificity of the effect. Each CST peptide inhibited I_{ACh} in a concentration-dependent manner (Fig. 3*D*). Consistent with their diminished catecholamine-release-inhibitory potencies (Fig. 2), CST-Ser-364 and CST-Val-367 peptides showed significantly lower I_{ACh} blocking effect as compared with CST-WT (Fig. 3*D*).

Third, we monitored the effect of each CST peptide on inhibition of a nicotine-evoked intracellular calcium ($[Ca^{2+}]_i$) rise in neuronally differentiated PC12 cells, as described recently (17). Representative traces of $[Ca^{2+}]_i$ under basal and nicotine-stimulated (in the presence/absence of each CST peptide) conditions are shown in Fig. 4. Each CST peptide blocked the nicotine-stimulated $[Ca^{2+}]_i$ although to different extents; in each case, the blocking effect was reversible upon application of nicotine to the cells (traces not shown). The extents of blockade of the $[Ca^{2+}]_i$ rise by the CST peptides at 5.0 μM were in the following order: CST-WT (~55%, n = 123 cells) > CST-Ser-364 (~44%, n = 103 cells) > CST-Val-367 (~39%, n = 90 cells). We also carried out a similar set of experiments in undifferentiated PC12 cells; the inhibitory effects on $[Ca^{2+}]_i$ rise were almost the same: CST-WT (~55%, n = 26 cells) > CST-Ser-364 (~44%, n = 30 cells) > CST-Val-367 (~38%, n = 25 cells).

Thus, at various stages of the nAChR signaling pathway (initial: agonist-evoked increase of inward Na^+ current; intermediate: agonist-evoked increase of intracellular free Ca^{2+} concentration; final: agonist-evoked exocytotic release of catecholamines), the naturally occurring CST variants displayed differential inhibitory effects in the same order.

The G364S Polymorphism and Plasma Catecholamine Concentrations—To investigate whether *in vivo* catecholamine secretion is altered between the carriers of Gly-364 and Ser-364 alleles, we measured their plasma norepinephrine and epinephrine levels. The G364S genotype groups differed in both norepinephrine (one-way ANOVA F = 6.648, p = 0.0017) and epinephrine (one-way ANOVA F = 5.109, p = 0.007) concentrations. The Gly/Ser and Ser/Ser carriers had lower level of norepinephrine (by ~27%, p = 0.0026 and 52%, p = 0.0001, respectively) than the Gly/Gly individuals (Fig. 5). The epinephrine level was also diminished (by ~30%, p = 0.0027) in Gly/Ser carriers (Fig. 5). Thus, the carriers of Ser-364 allele in our overall study population had lower plasma catecholamines. Of note, when the analysis was carried out only for healthy, normotensive subjects, the association of decreased catecholamine levels (by ~40%, p = 0.0002 for norepinephrine; by ~43%, p = 0.008 for epinephrine) with the Gly/Ser individuals (as compared with Gly/Gly individuals) prevailed (supplemental Table S1).

Differential Blockade of nAChR Desensitization by Human CST Variants—Besides its well studied antagonism to nAChR, catestatin also blocks agonist-induced desensitization of the receptor (15, 34). This phenomenon may increase the net catecholamine release into the circulation under circumstances of prolonged agonist exposure. Therefore, we tested whether the naturally occurring CST variants in our Indian study population exhibit differential blockade of nAChR desensitization evoked by repeated exposure to nicotine. Each CST variant enhanced desensitization-blocking effect (as measured by the extent of rise in catecholamine secretion after exposure of PC12 cells to nicotine for the second time) in a concentration-dependent manner (Fig. 6). Two-way ANOVA also revealed a significant interpeptide difference in their blockade of desensitization (and hence rise in catecholamine secretion) effect; the rank

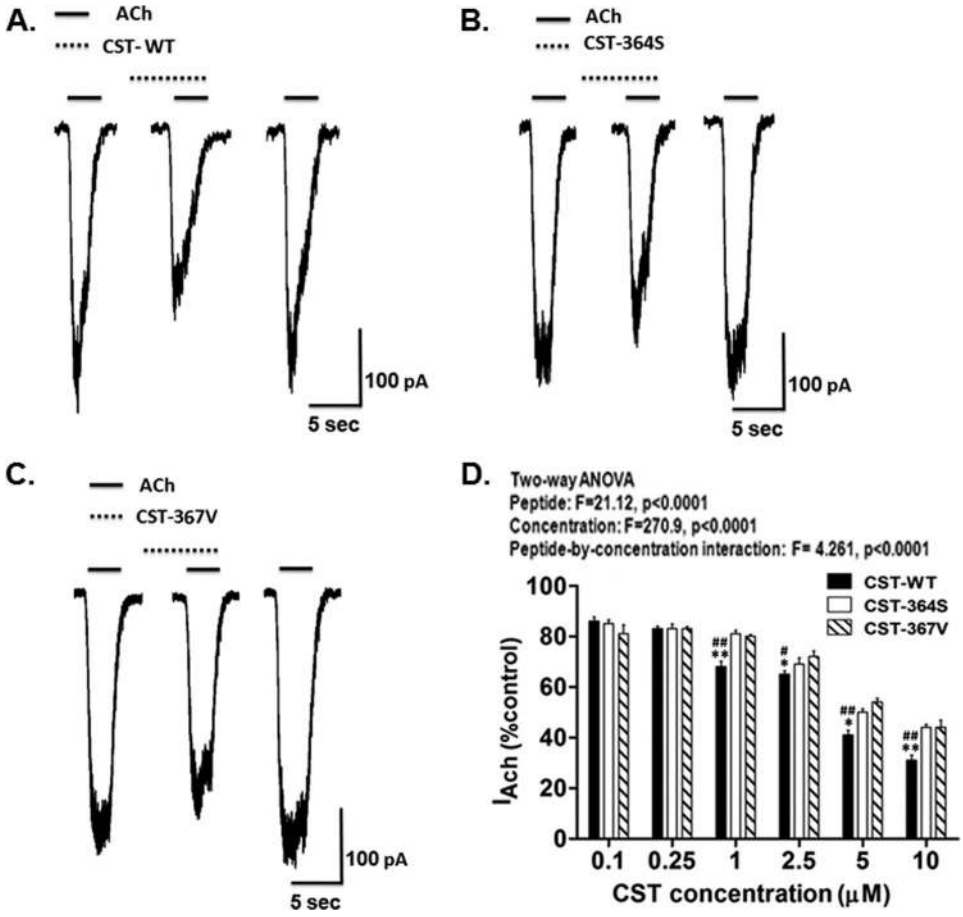

FIGURE 3. **CST variants differentially inhibit ACh-evoked inward current.** NGF-differentiated PC12 cells voltage-clamped at −80 mV were challenged with brief pulses (3 s) of ACh (100 μM) without/with CST peptides. *A*, *B*, and *C*, shown are representative traces for inhibition of inward current (I_{ACh}) by 5 μM CST-WT, CST-Ser-364, and CST-Val-367, respectively. The *solid horizontal bars above the traces* indicate the applications of ACh, and the *broken horizontal bars above the traces* indicate the applications of peptides in these experiments. *D*, the histogram shows inhibition of sodium currents by various CST peptides at different doses. Values are expressed as % of control I_{ACh} (*i.e.* inward current in the presence of ACh only) measured at the peak amplitude. Each point in the curves represents the mean ± S.E. of values obtained from nine cells. Results of two-way ANOVA are shown factoring for the effects of peptide, concentration, and peptide-by-concentration interaction on the I_{ACh}. * and ** indicate $p < 0.05$ and $p < 0.01$ with respect to CST-Ser-364, whereas # and ## indicate $p < 0.05$ and $p < 0.01$ with respect to CST-Val-367 (by two-tailed *t* test).

order of blockade, in general, was: CST-WT > CST-Ser-364 > CST-Val-367 (Fig. 6). This observation is consistent with the higher plasma norepinephrine concentration in Ser/Ser carriers than the Gly/Gly (*i.e.* wild type) carriers (Fig. 5) and suggests that the differential desensitization-blocking effect by CST variants may be one of the regulators of the ultimate circulating catecholamine levels *in vivo*.

Structural Basis for the Differential Actions of the CST Variants on nAChR—To probe whether there is a structural basis for the differences in the activities of CST variants, time-averaged structures of CST-WT, CST-Ser-364, and CST-Val-367 were generated. Molecular dynamics simulations showed that CST-Ser-364 and CST-Val-367 had significantly higher amounts of atomic level fluctuations than CST-WT, as evident from the root mean square deviation of C_α atoms and the root mean square fluctuation values (supplemental Fig. S1). Visualization of molecular dynamics trajectories also revealed profound differences in the propensities to adopt secondary structures in the following order: CST-WT (~73%) > CST-Ser-364 (~22%) > CST-Val-367 (~0.2%). Interestingly, whereas CST-WT and CST-Ser-364 adopt secondary structures comprising a 3_{10} helix and an anti-parallel β-sheet, CST-Val-367 lacks any helix (supplemental Fig. S2).

For verification of these computational structural predictions, we analyzed the secondary structure contents of the CST peptides by CD spectroscopy in physiological buffer (PBS, pH 7.4) with/without various percentages of TFE that are known to promote helix formation and provide membrane-mimicking environment. The CST peptides showed different extents of global secondary structure (as reflected by the minima at 208 nm and 222 nm in the spectra; Fig. 7); specifically, the propensity to assume α-helix was the highest for CST-WT and the least for CST-Val-367. For example, at 90% TFE, the helical content for CST-WT, CST-Ser-364, and CST-Val-367 were 20.4, 11.8, and 6.5%, respectively (Fig. 7, *panel D*). These observations correlate well with the computational predictions (supplemental Fig. S2).

To investigate whether alterations in the secondary structure of the peptides cause differential interactions with nAChR, docking of the CST structures on human $\alpha_3\beta_4$ nAChR subtype followed by molecular dynamics simulation was performed. The CST-WT peptide showed stronger interactions with the

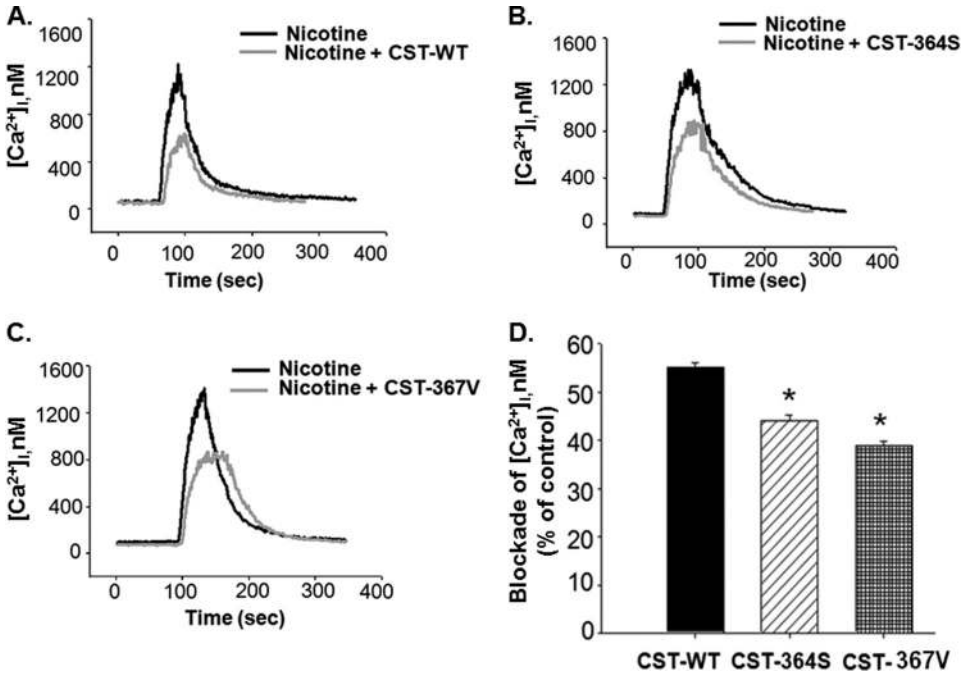

FIGURE 4. **CST variants block nicotine-evoked augmentation of cytosolic free calcium concentration.** NGF-differentiated PC12 cells loaded with Fura2-AM were stimulated with nicotine (200 μM) in the absence/presence of CST peptides (5.0 μM). The intracellular calcium concentration ($[Ca^{2+}]_i$) values were calculated from the Fura-2 fluorescence. *A*, *B*, and *C*, shown are representative $[Ca^{2+}]_i$ transients in the cases of nicotine (*black trace*) and CST-WT, CST-Ser-364, and CST-Val-367 (*gray traces*) respectively. *D*, the percentage blockade of $[Ca^{2+}]_i$ for each CST peptide was calculated. Data plotted are the mean ± S.E. values from 123 cells for CST-WT, 103 cells for CST-Ser-364, and 90 cells for CST-Val-367. One-way ANOVA followed by Gabriel post hoc tests between the groups suggested significant difference in blocking the nicotine-stimulated calcium rise among the peptides. * indicates $p < 0.05$ with respect to CST-WT.

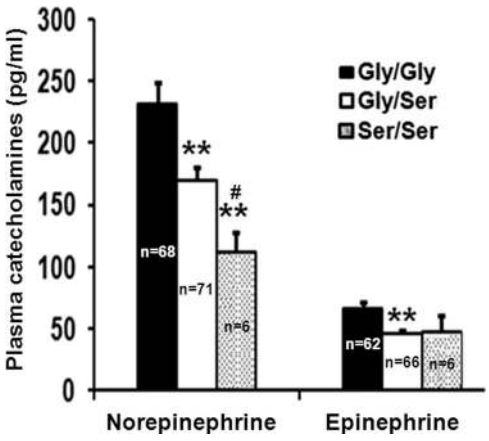

FIGURE 5. **Plasma catecholamine levels are diminished in the carriers of Ser-364 allele.** Norepinephrine and epinephrine concentrations in freshly thawed plasma samples were quantified by a radioimmunoassay kit according to the manufacturer's instructions, and the results are expressed in pg/ml. One-way ANOVA followed by Bonferroni post hoc test revealed that the Gly/Ser and the Ser/Ser carriers had significantly diminished levels of catecholamines than the Gly/Gly carriers. **, $p < 0.01$ with respect to Gly/Gly carriers; #, $p < 0.01$ with respect to Gly/Ser carriers. The number of samples tested for the different genotypes are shown.

human nAChR as compared with the CST-Ser-364 and CST-Val-367 peptides. Specifically, a large number of ionic interactions between CST-WT (involving the Lys-4, Arg-8, Arg-10, and Arg-15 residues) and human nAChR (involving Glu-17 from α_3-1, Asp-99, Asp-103, and Asp-104 from α_3-2, and Lys-80 from β_4-2) were observed (Fig. 8*A*). The CST-Ser-364 peptide had comparatively lower ionic interactions (that involved Lys-4, Arg-8, and Arg-15 residues) with the human nAChR (Asp-103 from α_3-1, Asp-103 and Asp-104 from α_3-2) (Fig. 8*B*). On the other hand, CST-Val-367 had no ionic interactions with the human nAChR, but it showed predominantly higher occurrence of hydrophobic interactions mostly clustered in the β_4-2 subunit of the human nAChR; CST-Val-367 (Gln-20 and Ser-1) also showed some hydrogen-bonding interactions with residues from other subunits of human nAChR (Arg-81 from β_4-1, Asp-104 from α_3-2, and Asp-94 from β_4-3) (Fig. 8*C*). Concomitant with such differential interactions with the receptor, the docking energy values for the CST peptides were in the following order: CST-WT (−19 kcal/mol) < CST-Ser-364 (−13 kcal/mole) < CST-Val-367 (−9 kcal/mole) (Fig. 9*A*). In addition, pore profile analysis at the extracellular vestibule of nAChR revealed different extents of occlusion by these CST peptides; the percentage occlusion of the pore (with respect to the free nAChR) was in the order: CST-WT (~85%) > CST-Ser-364 (~35%) > CST-Val-367 (~12%). Corroboratively, the minimum pore radius for the extracellular vestibule region of the nAChR before and after binding with the CST peptides were as follows: free nAChR (4.17 Å) > CST-Val-367 (3.66 Å) > CST-Ser-364 (2.77 Å) > CST-WT (0.63 Å) (Fig. 9*B*).

Thus, there is a strong co-relation between differential activities of the CST variants and their secondary structures. Specifically, the CST-WT peptide (perhaps, by virtue of much higher helical content) seems to exert stronger affinity to nAChR as well as greater occlusion of the receptor pore as compared with CST-Ser-364 and CST-Val-367.

The G364S Polymorphism and Circulating Glucose and Triglycerides Levels—To understand implications of the G364S variant (that occurred in ~15% of our study population) *in vivo*, we

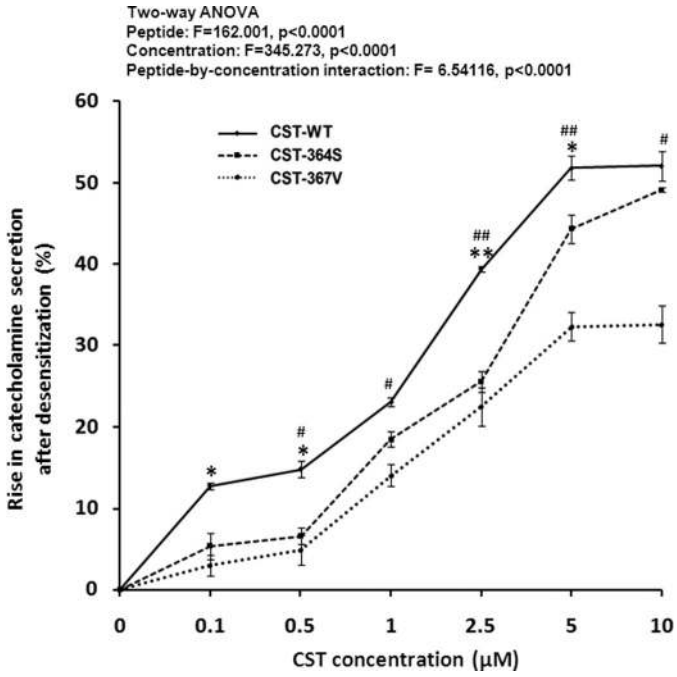

FIGURE 6. **Differential inhibition of nicotine-induced desensitization by CST variants.** PC12 cells preloaded with [^{3}H]norepinephrine were challenged with a concentration of 30 μM nicotine for 10 min with/without increasing concentrations (0.1–10 μM) of the CST variants. Cells were washed 2 times with secretion buffer and then rechallenged again with the agonist (30 μM nicotine) without peptides. After 10 min, cells were harvested for measurement of norepinephrine release in the media and cell lysate. Data were expressed as % increments (mean ± S.E.) in norepinephrine secretion due to CST peptides with respect to the untreated (without CST peptides) condition. Results of two-way ANOVA are shown, factoring for the effects of peptide, concentration, and peptide-by-concentration interaction on the norepinephrine secretion. * and ** indicate $p < 0.05$ and $p < 0.01$ with respect to CST-Ser-364, whereas # and ## indicate $p < 0.05$ and $p < 0.01$ with respect to CST-Val-367 (by two-tailed *t* test).

phenotyped the subjects for various parameters (Table 2) and carried out genotype-phenotype association analysis. The subjects were stratified by diploid genotypes: Gly/Gly major allele homozygotes, Gly/Ser heterozygotes, Ser/Ser minor allele homozygotes. The genotype groups did not differ in age, height, weight, and body mass index. The systolic blood pressure, diastolic blood pressure, mean arterial pressure, heart rate, left ventricular dimension at end diastole, and left ventricular dimension at end systole also did not differ significantly among the genotype groups. However, significant differences in the hemoglobin (one-way ANOVA F = 3.19, $p = 0.042$), plasma glucose (one-way ANOVA F = 5.64, $p = 0.004$), triglycerides (one-way ANOVA F = 5.54, $p = 0.004$), and HDL (one-way ANOVA F = 11.11, $p = 0.00002$) levels were observed among the three genotype groups. Whereas hemoglobin and HDL effect sizes were modest, glucose and triglyceride effect sizes were prominent; Gly/Ser individuals had ~4.5 mg/dl higher plasma glucose ($p = 0.001$ by Gabriel post hoc test, $p = 0.003$ by Hochberg post hoc test) and ~11 mg/dl higher triglycerides ($p = 0.0195$ by Gabriel post hoc test, $p = 0.0338$ by Hochberg post hoc test) than the Gly/Gly individuals (Table 2). Because our overall study population consisted of a large number of hypertensive subjects, we also analyzed the phenotypic data for Gly/Ser and Gly/Gly genotype groups after stratification of blood pressure status (supplemental Table S1). In only healthy, unmedicated, normotensive subjects did the Gly/Gly and Gly/Ser genotype groups significantly differ between plasma hemoglobin ($p = 0.039$), potassium ($p = 0.034$), and triglycerides ($p < 0.0001$) besides catecholamines; the plasma glucose level did not achieve statistical significance ($p = 0.095$), although the allele-specific effect size was higher (similar to the overall study population) in the carriers of the Ser allele (supplemental Table S1). Of particular mention is a profound elevation of triglycerides (by ~25 mg/dl) in the Gly/Ser individuals (as compared with the Gly/Gly individuals) in this healthy normotensive population. Thus, the Ser-364 allele, in general, was associated with several biochemical traits relevant for metabolic disorders.

Linkage Disequilibrium of the G364S Variant with Other Common CHGA SNPs—To test whether the G364S variant is likely to be inherited with other common functional (*i.e.* transcriptionally active) *CHGA* promoter SNPs (20), we resequenced an ~1-kb proximal promoter region in a subset of our study population. The -1018A→T (rs9658629), -415T→C (rs9658635), -57C→T (rs9658638) SNPs were observed to be the most common (with minor allele frequencies of 0.221, 0.368, and 0.236, respectively) promoter polymorphisms in our study population. Linkage disequilibrium analysis by Haploview 4.2 on the genotyped data for 333 subjects showed strong association of the G364S variant with each of these common promoter SNPs: $D' = 1.0$, LOD = 1.81, $r^2 = 0.02$ for -1018A→T; $D' = 1.0$, LOD = 4.71, $r^2 = 0.04$ for -415T→C; $D' = 1.0$, LOD = 1.48, $r^2 = 0.019$ for -57C→T. Additionally, we tested the association of the G364S variant with a nearby coding region variant G297S (rs 9658664) that is located within the dysglycemic peptide PST domain in exon 7 of *CHGA* because the rs 9658664 SNP appears to alter the risk for type 2 diabetes in an Indian population.[3] We had genotypic and phenotypic data for both CST G364S and PST G297S variants for 1010 individuals; the PST SNP (with minor allele frequency of 6.56%) displayed strong linkage disequilibrium with the CST SNP ($D' = 1.0$, LOD = 1.83, $r^2 = 0.006$).

DISCUSSION

In view of the recent studies providing evidence for cardiovascular/metabolic functions regulatory effects of CST (4, 35, 36), we sought to investigate functional genetic variations in this peptide in an Indian population. Resequencing of the CST region in the Indian study population yielded two non-synonymous variants: G364S and G367V (Table 1). Analysis of the sequence homology of the CST sequences across species showed that among mammals, the Gly residue at the 364-amino acid position of CHGA was absolutely conserved, whereas the Gly residue at 367 position was changed to Asp only in rodents (3). Interestingly, an earlier study in a Southern California population detected three non-synonymous variants in the CST domain: G364S, P370L, and R374Q (15). Thus, the present study discovered a novel CST variant (*viz.* G367V) and did not detect the P370L and R374Q variants. Moreover, the frequency of the minor allele Ser-364 in this Indian study pop-

[3] B. S. Sahu, J. M. Obbineni, G. Sahu, P. K. R. Allu, L. Subramanian, P. J. Sonawane, P. K. Singh, B. K. Sasi, S. Senapati, S. K. Maji, A. K. Bera, B. S. Gomathi, A. S. Mullasari, and N. R. Mahapatra, unpublished observation.

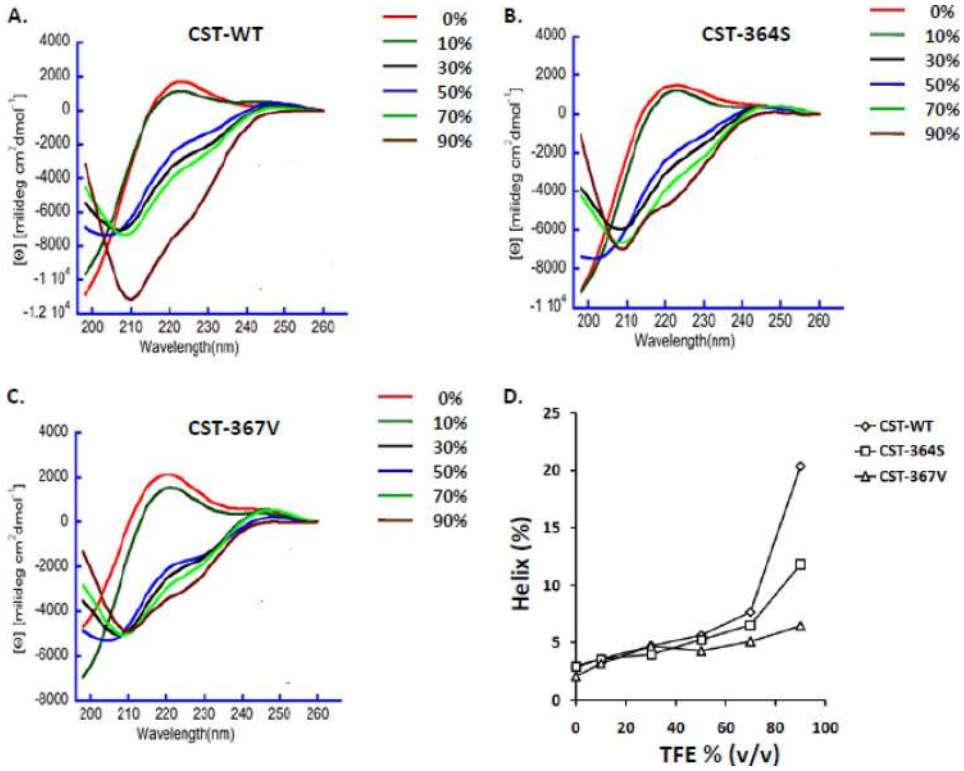

FIGURE 7. **CD spectra of the CST variants.** CD spectra of the human CST peptides (at 50 μM concentration in PBS, pH 7.4) were monitored over a 198–260 nm wavelength in the absence or presence of 10, 30, 50, 70, and 90% TFE. Ascending TFE concentrations induced α-helix formation, as indicated by the two minima at 208 and 222 nm. The representative traces for CST-WT (*A*), CST-Ser-364 (*B*), and CST-Val-367 (*C*) are shown. *D*, α-helix content for the CST peptides at various TFE concentrations is shown; the data were generated by deconvolution of spectra. The peptides showed altered propensities for formation of α-helix in the following order: CST-WT > CST-Ser-364 > CST-Val-367.

ulation (~8.0%) is much higher than the Southern California population (~3.1%). Of note, as per HapMap phase 3 data (www.ncbi.nlm.nih.gov) frequency of the Ser-364 allele in a Chinese population in Metropolitan Denver, Colorado (n = 82 subjects), was 7.3%, and that in a Gujarati Indian population in Houston, Texas (n = 87 subjects) was 6.9%; these values clearly are consistent with the frequency in our Indian study population (n = 1010 subjects), mostly consisting of South Indians; in contrast, the allele frequency was only 0.4% in a Maasai, Kinyawa, Kenya population (n = 142 subjects), 1.1% in a Luhya, Webuya, Kenya population (n = 87 subjects), and 2.4% in a Toscan, Italy population (n = 84 subjects). Thus, the CST domain of *CHGA* locus displays significant genetic variations between different ethnic populations, with a much higher occurrence of Ser-364 allele in South Asian populations.

Functional analysis of the synthesized human CST peptides (*viz.* CST-WT, CST-Ser-364 and CST-Val-367) revealed differential nAChR inhibitory effects at various stages of the nicotinic-cholinergic signaling in PC12 cells in a concentration-dependent manner (Figs. 2, 3, 4, and 6). In general, these peptides exhibited a modest nAChR blocking effect at ~100–500 nM concentrations, whereas the effect became more pronounced, and the interpeptide differences became significant at ≥1 μM concentration. Could such concentrations of these peptides be achieved *in vivo*? The concentration of the precursor protein CHGA in chromaffin granules/catecholamine storage vesicles has been reported to be ~4 mM (37–39), and the concentration of CHGA in the extracellular space in the vicinity of the exocytotic pore just after exocytosis is ~0.4 mM (11, 40). Thus, although the steady-state plasma concentration of these peptides may be in the nanomolar range, their concentrations in the vicinity of adrenal medullary chromaffin cells/sympathetic post-ganglionic neurons after its exocytotic release from the catecholamine storage vesicles are likely to be much higher (perhaps, in the micromolar range). Therefore, the nAChR inhibitory effects of these peptides involving an autocrine, negative-feedback mechanism (11, 41) may be physiologically relevant.

The Ser-364 allele was associated with profound changes in autonomic activity (increased baroreceptor slope during upward and downward deflections, increased cardiac parasympathetic index, decreased cardiac sympathetic index) in a small but age-, sex-, blood pressure status (only normotensives)-, weight-, height-, and body mass index-matched study population (consisting of n = 17 Gly/Ser and n = 48 Gly/Gly individuals) as compared with Gly-364 allele (21). Interestingly, the Ser-364 allele displayed association with diminished diastolic blood pressure levels only in males but not in females in a Southern California study population (21). However, the present study did not detect an association of this SNP with blood pressure. One possible reason for this difference between these two studies could be that the subjects in the Southern California study population were significantly older (mean age ~59 years) than the Indian study subjects (mean age ~39 years).

A major finding of this study is that subjects with both Gly/Ser and Ser/Ser genotypes displayed profoundly diminished (as

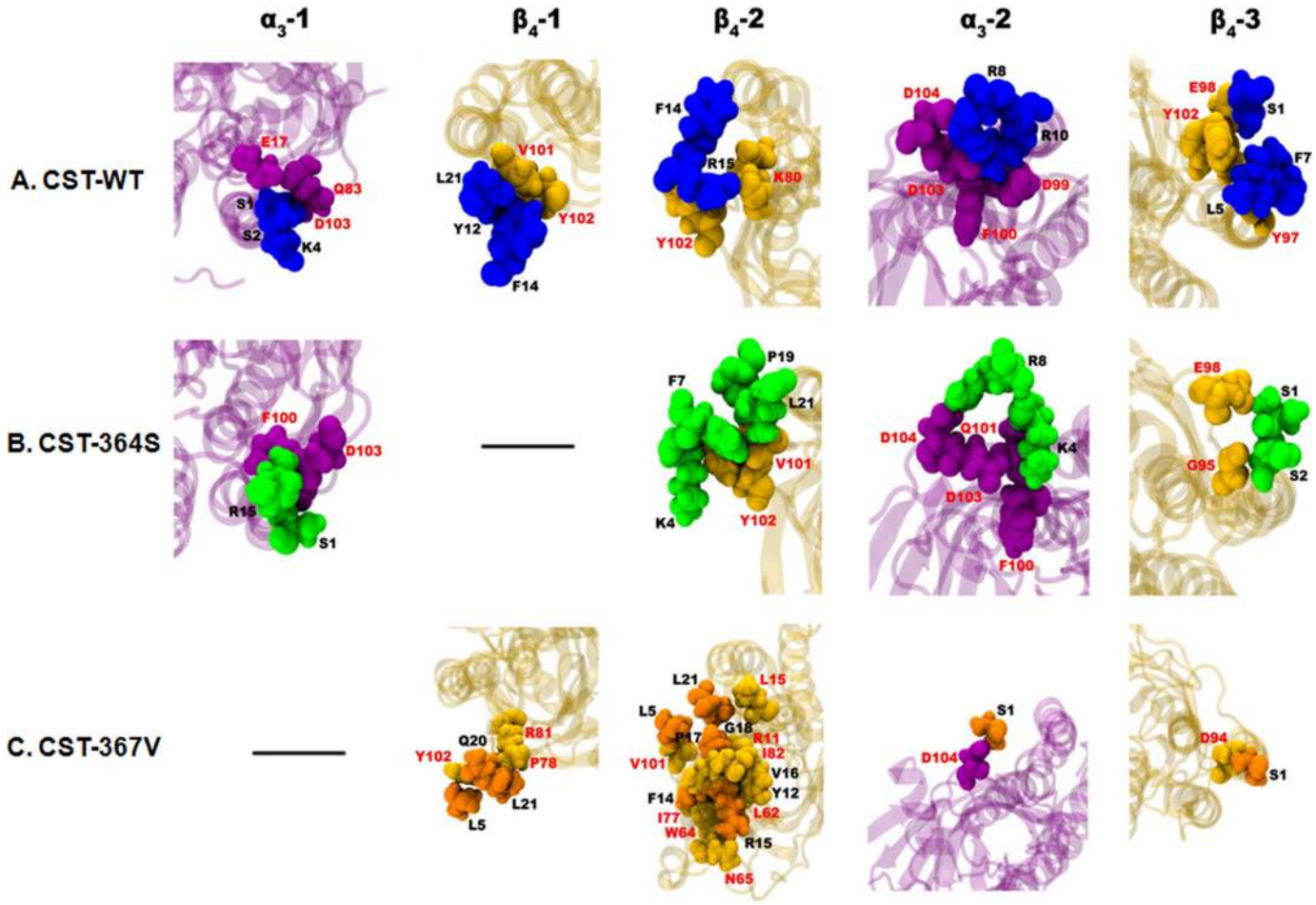

FIGURE 8. **Molecular interactions of CST variants with human nAChR.** Docking of the CST variants onto the $\alpha_3\beta_4$ nAChR followed by molecular dynamics simulations revealed interacting residues of each peptide and the receptor. *A*, interactions of the CST-WT peptide with the individual subunits of the receptor are shown. The CST-WT peptide is shown in *deep blue*, whereas α_3 and β_4 subunits are represented in *magenta* and *yellow*, respectively. Interactions existed with all the subunits of the pentameric structure of the receptor. *B*, shown are interactions of the human CST-Ser-364 peptide with the individual subunits of the receptor. The CST-Ser-364 peptide is shown in *green*, whereas α_3 and β_4 subunits are represented in *magenta* and *yellow*, respectively. Interestingly, the CST-Ser-364 did not show any interaction with the first β_4 subunit of the receptor. *C,* interactions of the human CST-Val-367 peptide with the individual subunits of the receptor are shown. The CST-Val-367 peptide is shown in *orange*, where α_3 and β_4 subunits are represented in *magenta* and *yellow*, respectively. Interestingly, the CST-Val-367 did not show any interaction with the first α_3 subunit of the pentameric nAChR.

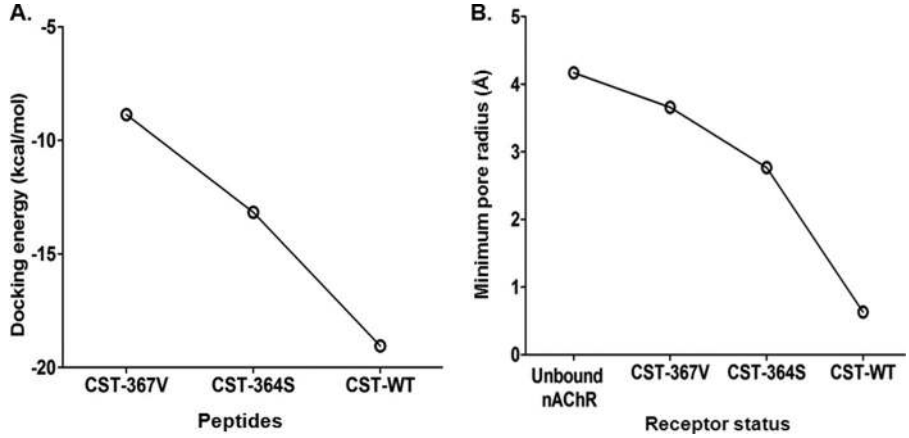

FIGURE 9. **CST variants have differential receptor binding affinity as well as receptor blockade.** *A*, shown is a docking energy pattern of the CST variants with the human $\alpha_3\beta_4$ nAChR. The docking energies for the peptides were in the following order: CST-WT (−19.05 kcal/mol) < CST-Ser-364 (−13.17 kcal/mol) < CST-Val-367 (−8.87 kcal/mol), suggesting that among these peptides interaction of CST-WT with the receptor is strongest that is followed by CST-Ser-364 and CST-Val-367, respectively. *B*, shown is a pore radius profile of the unbound and bound CST nAChR structures at the extracellular vestibule. CST-WT peptide showed minimum pore radius thereby creating minimum solvent accessible pathway through the pentameric ion channel corroborating with its highest potency for inhibition of channel function. The order of the minimum pore radius for the CST peptides bound to nAChR was as follows: free nAChR > CST-Val-367 > CST-Ser-364 > CST-WT.

TABLE 2

Demographic, physiological, and clinical characteristics of CST G364S genotypes

Data are presented as the mean ± S.E. BMI, body mass index; SBP, systolic blood pressure; DBP, diastolic blood pressure; MAP, mean arterial pressure; LVIDd, left ventricular dimension at end diastole; LVIDs, left ventricular dimension at end systole; The glucose values were random plasma glucose levels. Statistical significance for Gly/Ser and Ser/Ser genotypes were tested with respect to the Gly/Gly genotype. The significantly differing parameters are shown in bold.

Parameters	Gly/Gly	Gly/Ser	Ser/Ser
Demographic/Physical			
Age (years)	39.2 ± 0.3 (n = 858)	38.4 ± 0.8[a] (n = 144)	33.7 ± 2.6[a] (n = 8)
Sex (male/female)	67/33%	66/34%	56/44%
Hypertensives/normotensives	44/56%	47/53%	56/44%
Height (cm)	163.4 ± 0.3 (n = 858)	163.3 ± 0.7[a] (n = 144)	160.4 ± 2.9[a] (n = 8)
Weight (kg)	65.0 ± 0.3 (n = 858)	65.1 ± 0.9[a] (n = 144)	57.4 ± 2.5[a] (n = 8)
BMI (kg/m^2)	24.5 ± 0.2 (n = 858)	24.3 ± 2.6[a] (n = 144)	22.4 ± 1.3[a] (n = 8)
Physiological			
SBP (mm Hg)	139.6 ± 0.8 (n = 809)	142.6 ± 1.9[a] (n = 132)	134.0 ± 14.8[a] (n = 5)
DBP (mm Hg)	83.9 ± 0.4 (n = 809)	85.0 ± 1.0[a] (n = 132)	84 ± 7.5[a] (n = 5)
MAP (mm Hg)	102.3 ± 0.5 (n = 810)	104.7 ± 1.2[a] (n = 127)	100.6 ± 9.8[a] (n = 5)
Heart rate (beats/min)	76.6 ± 0.3 (n = 843)	76.2 ± 0.6[a] (n = 141)	72.4 ± 1.6[a] (n = 7)
LVIDd (mm)	44.7 ± 0.1 (n = 824)	45.1 ± 0.3[a] (n = 139)	45.1 ± 1.3[a] (n = 8)
LVIDs (mm)	27.1 ± 0.1 (n = 820)	27.5 ± 0.3[a] (n = 135)	27.2 ± 1.2[a] (n = 8)
Biochemical			
Hemoglobin (g/dl)	**13.3 ± 0.05 (n = 789)**	**13.6 ± 0.13[b] (n = 133)**	13.0 ± 0.33[a] (n = 7)
Sodium (meq/liter)	137.1 ± 0.2 (n = 799)	137.8 ± 0.3[a] (n = 129)	138.7 ± 1.3[a] (n = 8)
Potassium (meq/liter)	3.99 ± 0.01 (n = 795)	3.96 ± 0.02[a] (n = 133)	3.97 ± 0.09[a] (n = 7)
Urea (mg/dl)	24.0 ± 0.3 (n = 800)	24.9 ± 0.7[a] (n = 137)	23.4 ± 2.6[a] (n = 8)
Creatinine (mg/dl)	0.84 ± 0.01 (n = 807)	0.88 ± 0.01[a] (n = 137)	0.81 ± 0.07[a] (n = 7)
Glucose (mg/dl)	**93.2 ± 0.5 (n = 748)**	**97.7 ± 1.5[b] (n = 135)**	96.9 ± 10.9[a] (n = 7)
Total cholesterol (mg/dl)	167.4 ± 1.1 (n = 784)	165.4 ± 2.6[a] (n = 126)	170.0 ± 15.4[a] (n = 8)
Triglycerides (mg/dl)	**121.7 ± 1.7 (n = 695)**	**132.7 ± 4.5[b] (n = 131)**	**158.4 ± 19.4[b] (n = 8)**
HDL (mg/dl)	**37.3 ± 0.3 (n = 789)**	**38.2 ± 0.5[c] (n = 134)**	**49.2 ± 6.9[c] (n = 8)**
LDL (mg/dl)	99.8 ± 0.9 (n = 777)	103 ± 2.2[a] (n = 130)	83.6 ± 11.0[a] (n = 8)
Epinephrine (pg/ml)	**66.2 ± 5.5 (n = 62)**	**46.2 ± 2.8[b] (n = 66)**	47.0 ± 13.6[a] (n = 6)
Norepinephrine (pg/ml)	**231.6 ± 17.2 (n = 68)**	**169.7 ± 10.4[c] (n = 71)**	**111.1 ± 16.2[c] (n = 6)**

[a] Not significant.
[b] $p < 0.05$.
[c] $p < 0.01$.

much as ~2.1-fold with respect to Gly/Gly individuals) levels of plasma catecholamines (Fig. 5). This observation might seem paradoxical at the first glance because the CST-Ser-364 peptide is a less potent inhibitor of nicotinic/cholinergic-stimulated catecholamine secretion (Fig. 2; Ref. 15) than the CST-WT peptide. However, this can be explained by the fact that CST-Ser-364 is also a less potent inhibitor of desensitization of catecholamine secretion than CST-WT (Fig. 6; Ref. 15); conceivably, the net/cumulative effect of a CST peptide on the circulating catecholamine levels may significantly depend on its activity during the phenomenon of chronic/repeated exposure (*i.e.* desensitization) of the agonist on nAChR. Nevertheless, it must be noted that the plasma catecholamine levels in an individual would be determined by various other factors (*viz.* their biosynthesis, storage, and metabolism) apart from the contribution of the endogenous catecholamine release-inhibitory peptide CST. What might be the molecular basis for this diminished potency for CST-Ser-364? CD spectroscopy coupled with computational analysis of peptide structures (Fig. 7 and supplemental Fig. S2) revealed a significant reduction in helical content for CST-Ser-364; such alteration in the secondary structure was predicted to diminish interactions with nAChR (Figs. 8 and 9; Ref. 17). Notably, a previous study in a Southern California population (21) also detected a significant reduction (~1.6-fold) of plasma norepinephrine level (although plasma epinephrine level was unchanged, possibly due to a much smaller sample size as compared with this study) in Gly/Ser individuals than Gly/Gly subjects; however, both urinary nonepinephrine and epinephrine levels were declined by ~1.4- and ~1.5-fold, respectively, in Gly/Ser subjects). Thus, association of the Ser-364 allele with catecholamine secretion *in vivo* seems to replicate well in two geographically/ethnically distinct populations.

Beside catecholamines, the glucose and triglyceride levels were also significantly changed in the subjects carrying the CST Ser-364 allele. How might the Ser-364 allele alter the plasma glucose and triglyceride levels? Emerging data indicate that CST significantly inhibits hepatic glucose production, thereby acting as an insulin-like molecule in mice (4). Although mechanistic basis and relative efficacies/potencies of these CST variants on inhibiting gluconeogenesis is not yet known, CST-Ser-364 peptide might repress a key gluconeogenesis enzyme phosphoenol pyruvate carboxykinase (PEPCK) transcription to a lesser extent than the CST-WT in view of the recent report of protein kinase B (AKT, a repressor of PEPCK; Ref. 42) activation by CST via its interaction on β2-adrenergic receptor (12). The alteration in the plasma glucose level could also be due to/contributed by the non-synonymous SNP (*viz.* G297S) in the dysglycemic peptide PST (an inhibitor of insulin-stimulated glucose uptake; Ref. 43) that is in strong linkage disequilibrium with the CST G364S SNP. Likewise, CST has recently been reported to increase lipolysis (triglyceride hydrolysis) and lipid mobilization in adipose tissues via its interaction with α2-adrenergic receptor and leptin receptor (19). The higher triglyceride levels in subjects carrying the Ser-364 allele could be because of diminished lipolytic activity of this CST variant, perhaps due to lower antagonistic activity of the CST-Ser-364 peptide on α2-adrenergic receptor or lower activity on the leptin receptor similar to its nAChR-mediated catecholamine-release-inhibitory function. The higher triglyceride levels in the carriers of Ser-364 allele could also be mediated by the lower cat-

echolamines (Table 2) in those individuals as catecholamines are well known modulators of lipid profile. Intriguingly, the CST-Ser-364 peptide also displayed diminished potency (as compared with CST-WT) to regulate infarct size in the regionally ischemic-reperfused rat heart, likely to be mediated through a receptor(s) other than nAChR (44). Therefore, it appears that structural differences (*viz.* the extent of secondary structure) may govern the activities of CST peptides across various biological processes, mediated by different receptors.

In conclusion, we discovered two CST variants (G364S and G367V) in an Indian population. Our multidisciplinary (computational plus experimental) approach unraveled the mechanism of differential potencies of these CST peptides as compared with the wild type CST. This study also revealed that the presence of Ser-364 allele may alter the plasma levels of several important biochemical markers/traits (*viz.* catecholamines, glucose, triglycerides) for cardiovascular and metabolic physiology and pathophysiology and hence may alter the risk for future development of metabolic syndrome in a large section of human population.

Acknowledgments—We thank all individuals who voluntarily participated in this study. B. S. S. acknowledges Vinayak Gupta, Cardiovascular Genetics Lab, IIT Madras for help in this study. We are also thankful to the physician assistants T. Tamilselvi and M. Purrnima at the Madras Medical Mission hospital for excellent assistance. We also thank the High Performance Computing Facility at IIT Madras. We are grateful to Dr. V. Srinivasa Chakravarty, Department of Biotechnology, IIT Madras for providing a work station.

REFERENCES

1. Taupenot, L., Harper, K. L., and O'Connor, D. T. (2003) The chromogranin-secretogranin family. *N. Engl. J. Med.* **348,** 1134–1149
2. Belloni, D., Scabini, S., Foglieni, C., Veschini, L., Giazzon, A., Colombo, B., Fulgenzi, A., Helle, K. B., Ferrero, M. E., Corti, A., and Ferrero, E. (2007) The vasostatin-I fragment of chromogranin A inhibits VEGF-induced endothelial cell proliferation and migration. *FASEB J.* **21,** 3052–3062
3. Bartolomucci, A., Possenti, R., Mahata, S. K., Fischer-Colbrie, R., Loh, Y. P., and Salton, S. R. (2011) The extended granin family. Structure, function, and biomedical implications. *Endocr. Rev.* **32,** 755–797
4. Loh, Y., Cheng, Y., Mahata, S., Corti, A., and Tota, B. (2012) Chromogranin A and derived peptides in health and disease. *J. Mol. Neurosci.* **48,** 347–356
5. Kim, T., Tao-Cheng, J.-H., Eiden, L. E., and Loh, Y. P. (2001) Chromogranin A, an "on/off" switch controlling dense-core secretory granule biogenesis. *Cell* **106,** 499–509
6. Kim, T., and Loh, Y. P. (2005) Chromogranin A. A surprising link between granule biogenesis and hypertension. *J. Clin. Invest.* **115,** 1711–1713
7. Mahapatra, N. R., O'Connor, D. T., Vaingankar, S. M., Hikim, A. P., Mahata, M., Ray, S., Staite, E., Wu, H., Gu, Y., Dalton, N., Kennedy, B. P., Ziegler, M. G., Ross, J., and Mahata, S. K. (2005) Hypertension from targeted ablation of chromogranin A can be rescued by the human ortholog. *J. Clin. Invest.* **115,** 1942–1952
8. Angeletti, R. H., Aardal, S., Serck-Hanssen, G., Gee, P., Helle, K. B. (1994) Vasoinhibitory activity of synthetic peptides from the amino terminus of chromogranin A. *Acta Physiol. Scand* **152,** 11–19
9. Tota, B., Angelone, T., Mazza, R., and Cerra, M. C. (2008) The chromogranin A-derived vasostatins. New players in the endocrine heart. *Curr. Med. Chem.* **15,** 1444–1451
10. Sanchez-Margalet, V., Gonzalez-Yanes, C., Najib, S., and Santos-Ãlvarez, J. (2010) Metabolic effects and mechanism of action of the chromogranin A-derived peptide pancreastatin. *Regul. Pept.* **161,** 8–14
11. Mahata, S. K., O'Connor, D. T., Mahata, M., Yoo, S. H., Taupenot, L., Wu, H., Gill, B. M., and Parmer, R. J. (1997) Novel autocrine feedback control of catecholamine release. A discrete chromogranin A fragment is a noncompetitive nicotinic cholinergic antagonist. *J. Clin. Invest.* **100,** 1623–1633
12. Angelone, T., Quintieri, A. M., Brar, B. K., Limchaiyawat, P. T., Tota, B., Mahata, S. K., and Cerra, M. C. (2008) The antihypertensive chromogranin A peptide catestatin acts as a novel endocrine/paracrine modulator of cardiac inotropism and lusitropism. *Endocrinology* **149,** 4780–4793
13. Tota, B., Gentile, S., Pasqua, T., Bassino, E., Koshimizu, H., Cawley, N. X., Cerra, M. C., Loh, Y. P., and Angelone, T. (2012) The novel chromogranin A-derived serpinin and pyroglutaminated serpinin peptides are positive cardiac β-adrenergic-like inotropes. *FASEB J.* **26,** 2888–2898
14. Mahapatra, N. R., Mahata, M., Mahata, S. K., and O'Connor, D. T. (2006) The chromogranin A fragment catestatin. Specificity, potency, and mechanism to inhibit exocytotic secretion of multiple catecholamine storage vesicle co-transmitters. *J. Hypertens.* **24,** 895–904
15. Mahata, S. K., Mahata, M., Wen, G., Wong, W. B., Mahapatra, N. R., Hamilton, B. A., and O'Connor, D. T. (2004) The catecholamine release-inhibitory "catestatin" fragment of chromogranin A. Naturally occurring human variants with different potencies for multiple chromaffin cell nicotinic cholinergic responses. *Mol. Pharmacol.* **66,** 1180–1191
16. Herrero, C. J., Ales, E., Pintado, A. J., Lopez, M. G., Garcia-Palomero, E., Mahata, S. K., O'Connor, D. T., Garcia, A. G., and Montiel, C. (2002) Modulatory mechanism of the endogenous peptide catestatin on neuronal nicotinic acetylcholine receptors and exocytosis. *J. Neurosci.* **22,** 377–388
17. Sahu, B. S., Obbineni, J. M., Sahu, G., Singh, P. K., Sonawane, P. J., Sasi, B. K., Allu, P. K., Maji, S. K., Bera, A. K., Senapati, S., and Mahapatra, N. R. (2012) Molecular interactions of the physiological anti-hypertensive peptide catestatin with the neuronal nicotinic acetylcholine receptor. *J. Cell Sci.* **125,** 2323–2337
18. O'Connor, D. T.,Kailasam, M. T., Kennedy, B. P., Ziegler, M. G., Yanaihara, N., and Parmer, R. J. (2002) Early decline in the catecholamine release-inhibitory peptide catestatin in humans at genetic risk of hypertension. *J Hypertens.* **20**, 1335–1345
19. Bandyopadhyay, G. K., Vu, C. U., Gentile, S., Lee, H., Biswas, N., Chi, N.-W., O'Connor, D. T., and Mahata, S. K. (2012) Catestatin (chromogranin A(352–372)) and novel effects on mobilization of fat from adipose tissue through regulation of adrenergic and leptin signaling. *J. Biol. Chem.* **287,** 23141–23151
20. Wen, G., Mahata, S. K., Cadman, P., Mahata, M., Ghosh, S., Mahapatra, N. R., Rao, F., Stridsberg, M., Smith, D. W., Mahboubi, P., Schork, N. J., O'Connor, D. T., and Hamilton, B. A. (2004) Both rare and common polymorphisms contribute functional variation at CHGA, a regulator of catecholamine physiology. *Am. J. Hum. Genet.* **74,** 197–207
21. Rao, F., Wen, G., Gayen, J. R., Das, M., Vaingankar, S. M., Rana, B. K., Mahata, M., Kennedy, B. P., Salem, R. M., Stridsberg, M., Abel, K., Smith, D. W., Eskin, E., Schork, N. J., Hamilton, B. A., Ziegler, M. G., Mahata, S. K., and O'Connor, D. T. (2007) Catecholamine release-inhibitory peptide catestatin (chromogranin A(352–372)). Naturally occurring amino acid variant G364S causes profound changes in human autonomic activity and alters risk for hypertension. *Circulation* **115,** 2271–2281
22. Preece, N. E., Nguyen, M., Mahata, M., Mahata, S. K., Mahapatra, N. R., Tsigelny, I., and O'Connor, D. T. (2004) Conformational preferences and activities of peptides from the catecholamine release-inhibitory (catestatin) region of chromogranin A. *Regul. Pept.* **118,** 75–87
23. Simmerling, C., Strockbine, B., and Roitberg, A. E. (2002) All-atom structure prediction and folding simulations of a stable protein. *J. Am. Chem. Soc.* **124,** 11258–11259
24. Humphrey, W., Dalke, A., and Schulten, K. (1996) VMD. Visual molecular dynamics. *J. Mol. Graph.* **14,** 33–38
25. Morris, G. M., Goodsell, D. S., Halliday, R. S., Huey, R., Hart, W. E., Belew, R. K., and Olson, A. J. (1998) Automated docking using a Lamarckian genetic algorithm and an empirical binding free energy function. *J. Comput. Chem.* **19,** 1639–1662
26. Unwin, N. (2005) Refined structure of the nicotinic acetylcholine receptor at 4A resolution. *J. Mol. Biol.* **346,** 967–989
27. Barrantes, F. J. (2004) Structural basis for lipid modulation of nicotinic acetylcholine receptor function. *Brain Res. Rev.* **47,** 71–95

28. Brannigan, G., Hénin, J., Law, R., Eckenhoff, R., and Klein, M. L. (2008) Embedded cholesterol in the nicotinic acetylcholine receptor. *Proc. Natl. Acad. Sci. U.S.A.* **105,** 14418–14423
29. Phillips, J. C., Braun, R., Wang, W., Gumbart, J., Tajkhorshid, E., Villa, E., Chipot, C., Skeel, R. D., Kalé, L., and Schulten, K. (2005) Scalable molecular dynamics with NAMD. *J. Comput. Chem.* **26,** 1781–1802
30. Tina, K. G., Bhadra, R., and Srinivasan, N. (2007) PIC: Protein interactions calculator. *Nucleic Acids Res.* **35,** W473–W476
31. Smart, O. S., Goodfellow, J. M., and Wallace, B. A. (1993) The pore dimensions of gramicidin A. *Biophys. J.* **65,** 2455–2460
32. Cui, J. S., Hopper, J. L., and Harrap, S. B. (2003) Antihypertensive treatments obscure familial contributions to blood pressure variation. *Hypertension* **41,** 207–210
33. Mahata, S. K., Mahata, M., Fung, M. M., and O'Connor, D. T. (2010) Catestatin. A multifunctional peptide from chromogranin A. *Regul. Pept.* **165,** 52–62
34. Mahata, S. K., Mahata, M., Parmer, R. J., and O'Connor, D. T. (1999) Desensitization of catecholamine release. The novel catecholamine release-inhibitory peptide catestatin (chromogranin A-(344–364)) acts at the receptor to prevent nicotinic cholinergic tolerance. *J. Biol. Chem.* **274,** 2920–2928
35. Helle, K. B. (2010) Regulatory peptides from chromogranin A and secretogranin II. *Cell Mol. Neurobiol.* **30,** 1145–1146
36. Mahapatra, N. R. (2008) Catestatin is a novel endogenous peptide that regulates cardiac function and blood pressure. *Cardiovasc. Res.* **80,** 330–338
37. Benedum, U. M., Baeuerle, P. A., Konecki, D. S., Frank, R., Powell, J., Mallet, J., and Huttner, W. B. (1986) The primary structure of bovine chromogranin A. A representative of a class of acidic secretory proteins common to a variety of peptidergic cells. *EMBO J.* **5,** 1495–1502
38. Iacangelo, A., Affolter, H. U., Eiden, L. E., Herbert, E., and Grimes, M. (1986) Bovine chromogranin A sequence and distribution of its messenger RNA in endocrine tissues. *Nature* **323,** 82–86
39. Winkler, H., Apps, D. K., and Fischer-Colbrie, R. (1986) The molecular function of adrenal chromaffin granules. Established facts and unresolved topics. *Neuroscience* **18,** 261–290
40. Wightman, R. M. (1995) 8th *International Symposium on Chromaffin Cell Biology*, Edinburgh, Scotland S-25, 66, 6th–10th August 1995, International Society for Chromaffin Cell Biology
41. Mahata, S. K., Mahata, M., Wakade, A. R., and O'Connor, D. T. (2000) Primary structure and function of the catecholamine release inhibitory peptide catestatin (chromogranin A (344–364)). Identification of amino acid residues crucial for activity. *Mol. Endocrinol.* **14,** 1525–1535
42. Ono, H., Shimano, H., Katagiri, H., Yahagi, N., Sakoda, H., Onishi, Y., Anai, M., Ogihara, T., Fujishiro, M., Viana, A. Y., Fukushima, Y., Abe, M., Shojima, N., Kikuchi, M., Yamada, N., Oka, Y., and Asano, T. (2003) Hepatic Akt activation induces marked hypoglycemia, hepatomegaly, and hypertriglyceridemia with sterol regulatory element binding protein involvement. *Diabetes* **52,** 2905–2913
43. Zhang, K., Rao, F., Wen, G., Salem, R. M., Vaingankar, S., Mahata, M., Mahapatra, N. R., Lillie, E. O., Cadman, P. E., Friese, R. S., Hamilton, B. A., Hook, V. Y., Mahata, S. K., Taupenot, L., and O'Connor, D. T. (2006) Catecholamine storage vesicles and the metabolic syndrome. The role of the chromogranin A fragment pancreastatin. *Diabetes Obes. Metab.* **8,** 621–633
44. Brar, B. K., Helgeland, E., Mahata, S. K., Zhang, K., O'Connor, D. T., Helle, K. B., and Jonassen, A. K. (2010) Human catestatin peptides differentially regulate infarct size in the ischemic-reperfused rat heart. *Regul. Pept.* **165,** 63–70